DEFECT LAW OF CU/CO PATTERNED WAFERS AFTER USING A NOVEL BULK/BARRIER SLURRY AND CLEANING SOLUTION

Lifei Zhang[1], *Tongqing Wang*[1], *and Xinchun Lu*[1*]
[1]State Key Laboratory of Tribology, Tsinghua University, Beijing 100084, China
*Corresponding Author's Email: xclu@tsinghua.edu.cn

ABSTRACT

As feature size shrinks to 7 nm and beyond, cobalt (Co) has been applied as one of the most promising alternatives of diffusion barrier layers to be employed in copper (Cu) interconnects. The present work describes the defect law of Cu/Co patterned wafers after using a novel bulk/barrier slurry and cleaning solution during chemical mechanical polishing (CMP) and post-CMP cleaning process. The novel slurry and cleaning solution were mainly composed of potassium persulfate (KPS) as an oxidizer and citric acid as a complexing agent, respectively. With the changes of different line width, line space and pattern density, the defects including copper dishing, dielectric erosion, fang as well as particle residues were investigated.

INTRODUCTION

As device dimensions continue to decrease, Co has been emerged as one of the most promising candidates to be employed in Cu interconnects as a diffusion barrier layer[1]. Compared with the traditional Ta/TaN diffusion bilayers, Co shows an excellent gap-fill attribute, the capability of Cu directly electroplating as well as the conformal adhesion property with its relatively low resistivity. However, the integration of Cu and Co demands the compatibility with various wet process treatments, such as CMP and post-CMP cleaning process.

In our previous work, we have proposed a relatively stable KPS based barrier slurry and compared this KPS slurry with the conventional hydrogen peroxide based one[2]. It was found that 10 mM KPS with 3 vol.% colloidal silica could produce a material removal rate (MRR) selectivity of ~1 between Cu and Co films. On this basis, the coordination of different complexing agents and corrosion inhibitors with KPS has been studied in this research. Furthermore, it is remarkably that the polished Cu/Co surfaces could become inevitably contaminated by a large number of particles. It was demonstrated that citric acid could be used to remove silica particles from Cu and Co wafers[3], [4]. So, in this study, the citric acid cleaning solution has also been employed in Cu/Co patterned wafers to verify its cleaning ability.

Thus, a comprehensive study has been carried out to explore not only for the CMP process of Cu/Co patterned wafers, but also for the post CMP cleaning process. The objective of our research is to investigate the defect law of Cu/Co patterned wafers after using a novel KPS bulk/barrier slurry and citric acid cleaning solution.

EXPERIMENTAL

Cu films (~1.5 μm) and Co films (90 nm) were deposited on 50 mm silicon wafers as blanket wafers, respectively. A specific kind of patterned wafers which has different line width and space was used in this study. The mask floor plan and cross-sectional view of this kind of patterned wafers are shown in Figure 1. The selection of complexing agents mainly included citric acid (CA), glycine (GLY), and ethylenediamine tetraacetic acid (EDTA). Besides, 1,2,4- triazole (TAZ), potassium oleate (PO) as well as 1-Phenyl-1H-tetrazole-5-thiol (PMTA) were chosen to be the corrosion inhibitors.

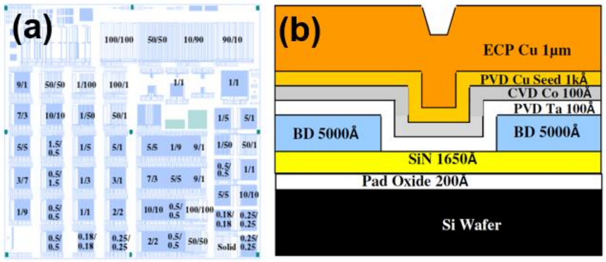

Figure 1: (a)SKW 5-3.18 mask floor plan, (b) cross-sectional view of the Cu/Co patterned wafers

EFFECTS OF COMPLEXING AGENTS AND INHIBITORS ON MRRS

The MRRs of Cu and Co wafers in the presence of 10 mM KPS at pH 10 with different complexing agents (5 mM) were shown in Figure 2(a). A relatively high Cu MRR (1924.5 Å/min) can be observed when GLY works as a complexing agent with KPS. Since the superfluous Cu is supposed to be removed rapidly during the first step, GLY was selected to be the complexing agent in the KPS bulk slurry. On the other hand, to reduce copper dishing and other defects, the barrier slurry requires to make sure the removal selectivity between Cu and Co, which means the MRR of Cu couldn't be too fast. As a result, CA is the most suitable complexing agent in the KPS barrier slurry.

On the foundation of KPS and CA, the effect of different inhibitors (5 mM) on Cu/Co MRRs in the barrier slurry is presented in Figure 2(b). TAZ and PO have a certain inhibition effect on the MRRs of Cu and Co, while the MRR of Cu is still higher than that of Co. On the contrary, when PMTA is applied as the inhibitor, the MRR of Cu (113.6 Å/min) is hindered, along with a promoted removal rate of Co (475.0 Å/min), which could effectively reduce the risk of copper dishing defects.

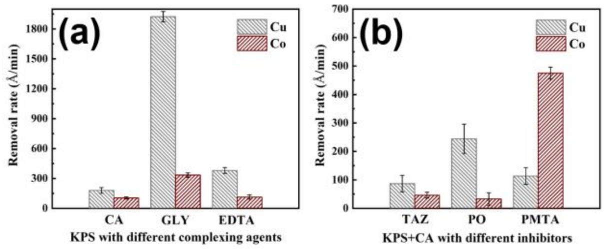

Figure 2: The effect of different (a) complexing agents and (b) inhibitors on Cu/Co MRRs in the KPS based slurry

INHIBITION EFFICIENCY OF DIFFERENT CORROSION INHIBITORS

A set of potentiodynamic polarization plots of Co with different inhibitors and concentrations was presented in Figure 3. With the concentration of TAZ and PO raising from 1 to 7 mM, the corrosion current density (Icorr) of Co continuously dropped. While with the increasing addition of PMTA, the Icorr of Co is much higher than that without PMTA, which explains the reason of enhanced Co MRR. The calculation of inhibition efficiency (θ) of each inhibitor was performed by the below equation:

$$\theta = 1 - \frac{I_{corr,with\ inhibitors}}{I_{corr,without\ inhibitors}} \times 100\% \qquad (1)$$

Aided by the computed θ, the adsorption behaviors of inhibitors on Cu and Co surfaces can be analyzed with the adsorption isotherm. For example, a liner relationship between Co surface coverage (equals inhibition efficiency, θ) and the concentration of inhibitor PO (c_i) can be obtained by using Langmuir adsorption isotherm, as shown in Figure 4. The Langmuir adsorption isotherm can be written as[5]:

$$\frac{c_i}{\theta} = c_i + \frac{1}{K} \qquad (2)$$

$$K = \frac{1}{55.5} \exp\left(-\frac{\Delta G_{ads}^0}{R_0 T}\right) \qquad (3)$$

where K is the adsorption equilibrium constant, ΔG_{ads}^0 is the Gibbs energy of adsorption, R_0 is the universal gas constant and T is the absolute temperature. When the PO actioned as the corrosion inhibitor for Co wafers, the calculated ΔG_{ads}^0 is equal to -27.23 KJ/mol, which indicates that PO is spontaneously adsorbed on the Co surfaces. Besides, the value of ΔG_{ads}^0 on the order of -20 KJ/mol or higher represents physisorption behavior, while the value of ΔG_{ads}^0 is around -40 KJ/mol or lower expresses that the adsorption is via the form of chemisorption. Based on the calculation, the adsorption of PO on Co wafers can be analyzed, which is the combination of physisorption (major) and chemisorption. The adsorption behaviors of the other two inhibitors on Cu and Co surfaces can be achieved by the same method.

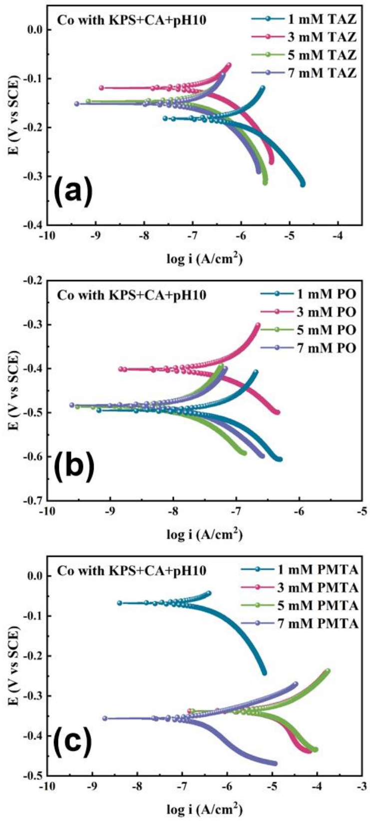

Figure 3: Potentiodynamic polarization plots of Co in the solution containing 10 mM KPS and 5 mM CA with different concentrations of (a) TAZ, (b) PO, (c) PMTA

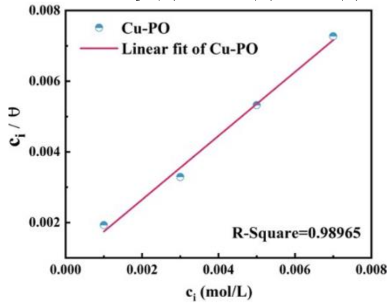

Figure 4: Langmuir isotherm plot for Co with inhibitor PO

To further explore and verify the adsorption behaviors, the XPS analysis of Co treated in different inhibitors was carried out, as shown in Figure 5. The reference curve presents the XPS spectra of the original Co surface. The XPS peaks which located at 61.1, 103.2, 780.8, 796.7, 927.9 eV are attributed to Co 3p, Co 3s, Co $2p_{3/2}$, Co $2p_{1/2}$, and Co 2s, respectively. With the addition of CA, the peaks of Co 2p and Co LMM increase, indicating the native oxide of Co was removed by complexation reaction. On this basis, N 1s appears when

TAZ and PMTA were added, while the enhanced C 1s comes into view with the addition of PO. These results proved that the three kinds of inhibitors are indeed absorbed or reacted on Co surfaces.

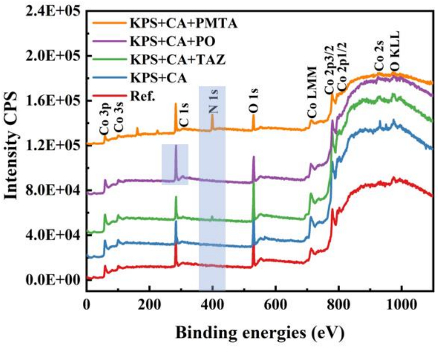

Figure 5: XPS spectra of Co surfaces treated by different solution

DEFECT LAW OF CU/CO PATTERNED WAFERS AFTER POLISHING

TABLE I. THE COMPONENTS OF BULK/BARRIER SLURRY AND CLEANING SOLUTION

Solution	Components
Bulk slurry	Silica, KPS, GLY, pH 10
Barrier slurry A	Silica, KPS, CA, pH 10
Barrier slurry B	Silica, KPS, CA, PMTA, pH 10
Cleaning solution A	CA, pH 11
Cleaning solution B	CA, PMTA, pH 11

TABLE II. DIFFERENT COMBINATIONS OF CMP AND POST CMP CLEANING PROCESS

Experiment number	Combinations of CMP and post CMP cleaning process
#1	Bulk slurry
#2	Bulk slurry + Barrier slurry A
#3	Bulk slurry + Barrier slurry B
#4	Bulk slurry + Barrier slurry B + Cleaning solution A
#5	Bulk slurry + Barrier slurry B + Cleaning solution B

Table I and II shown below summarize the specific components of the employed solution as well as different combinations of CMP and post CMP cleaning procedure. The SEM images of x/x arrays in Cu/Co patterned wafers after using the KPS bulk slurry are shown in Figure 6. It can be clearly seen that a large amount of silica particles has remained on the patterned surfaces after polishing. Besides, a severe corrosion phenomenon can be observed at the junction between Cu line, Co barrier layer and the dielectric material. The reason is the standard equilibrium potentials difference between Cu and Co, which will cause galvanic corrosion in the presence of multiple slurry components.

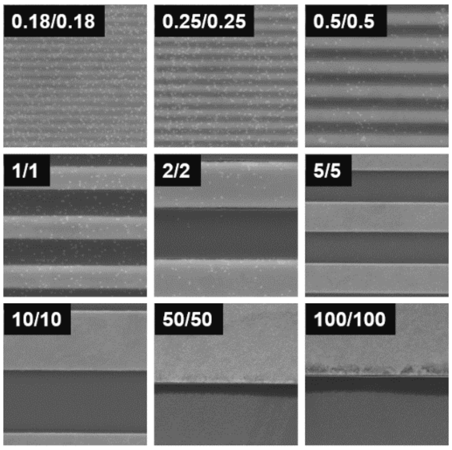

Figure 6: SEM images of x/x arrays after polishing using the KPS bulk slurry (line witdth $\leq 2\ \mu m$, 40 kX magnification; line witdth $\geq 5\ \mu m$, 40 kX magnification)

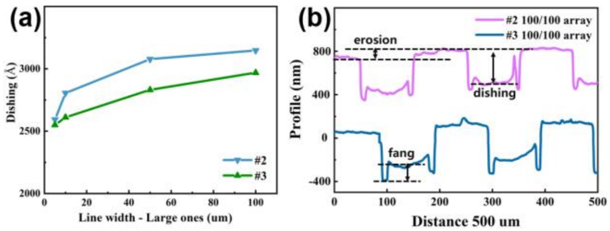

Figure 7: (a) changes of x/x arrays dishing with large line width, (b) defect comparison of 100/100 μm array after using different barrier slurry

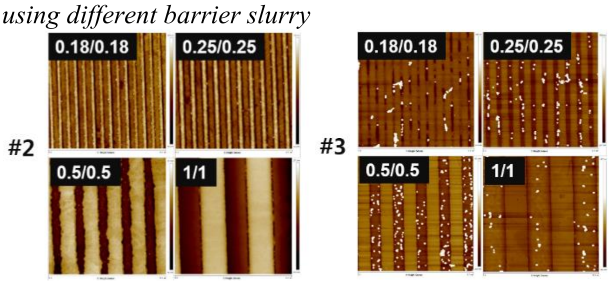

Figure 8: Topographic AFM images of x/x arrays with small line width after using different barrier slurry

The copper dishing results of x/x arrays with large line width after using two kinds of barrier slurry are presented in Figure 7(a). Copper dishing deteriorates gradually as the line width becomes larger. The main reason is that the polishing pad will deform a certain amount during the CMP process, and it is easier to bend towards the softer material, which is copper interconnect line. Meanwhile, the copper line with larger line width allows greater deformation, causing a bigger dishing defect. Besides, the comparison between #2 and #3 shows that the addition of PMTA in barrier slurry can improve the dishing defects. Figure 7(b) shows the line profiles of 100/100 μm array in #2 and #3. The barrier slurry without PMTA could give rise to the more serious erosion (935.0 Å), owing to the greater dishing and deformation. On the contrary, the barrier slurry containing PMTA leads to the deeper fang defect (1177.1 Å). The AFM images of the copper patterned structures with small line width after experiment #2 and #3 are shown in Figure 8. Obviously, the defect law of copper dishing is as same as the large line width arrays. However, compared with the barrier slurry without PMTA, the apparent particle residues after using the slurry containing PMTA indicate that it will weaken the ability of KPS and CA to impede the particle adsorption.

Figure 9 shows the dishing defect values of pattern density (PD). Taking #2 experiment as an example, when the conditions are PD<50% and consistent line width (such as 1/3 μm, 1/5 μm, 1/9 μm arrays), the copper dishing remains basically unchanged at 210.0 Å. Besides, the copper dishing values rise by degrees with the conditions of PD<50% and increasing line width. On the other hand, when PD is greater than 50%, regardless of the change of line space, the dishing values show an upward trend with the increment of line width. Also, the magnitude of dishing values of the PD>50% case is much greater than that of the array with PD<50%.

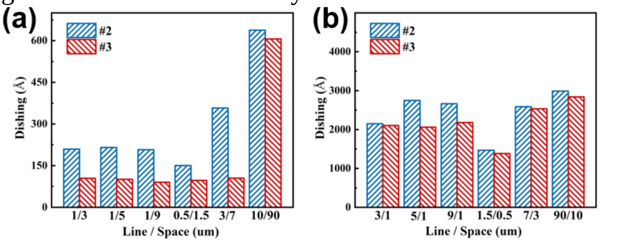

Figure 9: Changes of copper dishing with (a) PD<50%, (b) PD>50% arrays after using different barrier slurry

DEFECT LAW OF CU/CO PATTERNED WAFERS AFTER CLEANING

The defect law of Cu/Co patterned wafers after two steps polishing and post cleaning process is shown in Figure 10(a). From the changes of dishing values, it can be found that the copper dishing becomes severer with the addition procedure of post cleaning. Similarly, the larger the line width, the more obvious the rising range of the copper dishing, and the greater the defect value caused by cleaning solution without PMTA. Figure 10(b) presents the defect comparison of 100/100 μm array after employing two kinds of CA cleaning solution. The CA cleaning solution can not eliminate the influence of polishing slurry on dishing and fang defect. Meanwhile, the addition of PMTA in CA cleaning solution displays the same effect on patterned wafers, which can increase the fang value slightly.

Figure 11 shows the AFM images of x/x arrays with small line width after using two kinds of CA cleaning solution. Compared with the polished surfaces, the adhesive silica particles on the patterned structures are greatly reduced by the cleaning effect of CA solution. As a result, CA solution can effectively remove the silica particles which residue on the Cu/Co patterned surfaces after polishing. And the addition of PMTA can reduce the risk of copper dishing on the premise of meeting the same cleaning effect.

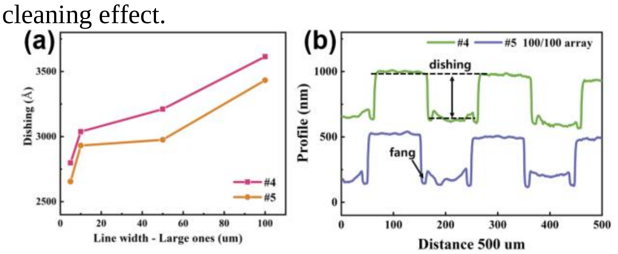

Figure 10: (a) changes of x/x arrays dishing with large line width, (b) defect comparison of 100/100 μm array after using different barrier slurry

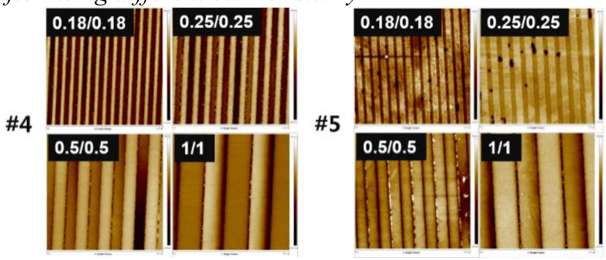

Figure 11: Topographic AFM images of x/x arrays with small line width after using different cleaning solution

CONCLUSIONS

The defect law of Cu/Co patterned wafers with different line width, space and pattern density was studied. Regardless of the line space and PD, the values of dishing and erosion defect show an upward trend with the increment of line width. Also, the growth magnitude of the PD>50% arrays is much greater than that of PD<50%. Furthermore, the addition of PMTA in the KPS barrier slurry as well as CA cleaning solution could reduce the risk of copper dishing and dielectric erosion, while it will slightly lead to the fang defect. It can also be concluded that citric acid could remove a certain number of silica particles on Cu/Co patterned wafers.

REFERENCES

[1] C. Yang, P. Flaitz, B. Li, F. Chen, C. Christiansen, S. Lee, P. Ma, D. Edelstein. *Microelectron. Eng.*, vol. 12, 2012, pp. 79-82.
[2] L. Zhang, T. Wang, X. Lu. *J. Mater. Sci.*, vol. 55, 2020, pp. 8992-9002.
[3] L. Zhang, T. Wang, X. Lu. *Microelectron. Eng.*, vol. 216, 2019, pp. 111090.
[4] L. Zhang, T. Wang, X. Lu. *Mater. Chem. Phys.*, vol.

275, 2022, pp. 125199.
[5] M. Hosseini, S. Mertens, M. Ghorbani, M. Arshadi. *Mater. Chem. Phys.*, vol. 78, 2003, pp. 800–808.